PHYSICAL REVIEW A VOLUME 59, NUMBER 5 MAY 1999

Oscillator strengths and electron-excitation cross sections for atomic nitrogen

S. S. Tayal and C. A. Beatty
Department of Physics, Clark Atlanta University, Atlanta, Georgia 30314

(Received 1 October 1998; revised manuscript received 4 January 1999)

The *LS* states belonging to the configurations $2s^22p^3$, $2s2p^4$, $2s^22p^23s$, $2s^22p^23p$, $2s^22p^23d$, and $2s^22p^24s$ of neutral nitrogen are considered in the calculations of excitation energies and oscillator strengths. Extensive configuration interaction wave functions are used, which give excitation energies in close agreement with the experiment. The calculation of the differential and integral cross sections of the forbidden $^4S^o$-$^2D^o$ transition for the scattering of electrons from atomic nitrogen is performed in a 11-state close-coupling approximation using the *R*-matrix method in the energy region from threshold to 70 eV. The calculated differential cross sections are peaked in the backward direction and compare very well with the recent measurement. The present integral cross sections also show very good agreement with the available other calculations and measurement. [S1050-2947(99)10205-1]

PACS number(s): 34.80.Dp

I. INTRODUCTION

Atomic collision and radiative processes play an important role in the understanding of energy balance and the rate of radiative decay in various types of plasmas and to determine theoretical line intensity ratios that eventually can be used to infer electron temperature, density, and elemental abundances in astrophysical plasmas. The determination of atomic transition probabilities and oscillator strengths for electric-dipole-allowed and intercombination transitions of nitrogen has been the subject of numerous experimental and theoretical studies. Recently Robinson and Hibbert [1], Hibbert *et al.* [2,3], and Tong *et al.* [4] reported extensive theoretical calculations of energy levels, oscillator strengths, and radiative lifetimes of excited states using the configuration-interaction (CI) method. Tong *et al.* [4] calculated oscillator strengths of electric-dipole-allowed transitions among the low-lying states of quartet symmetry in N I. Hibbert *et al.* [2,3] published oscillator strengths for a large number of electric-dipole-allowed and intercombination transitions between the quartet and doublet symmetry states belonging to the $2s^22p^3$, $2s2p^4$, $2s^22p^23s$, $2s^22p^23p$, $2s^22p^23d$, and $2s^22p^24s$ configurations of neutral nitrogen. Robinson and Hibbert [1] calculated oscillator strengths for the four resonance transitions from the $2s^22p^3\,{}^4S^o$ state to the $2s^22p^23s\,{}^4P$, $2s2p^4\,{}^4P$, $2s^22p^24s\,{}^4P$, and $2s^22p^23d\,{}^4P$ states of N I within the framework of nonorthogonal orbitals. Bell and Berrington [5] used *R*-matrix method to calculate oscillator strengths of dipole-allowed transitions between the $^4S^o$ and ^4P states.

On the experimental side oscillator strengths of seven lines of N I belonging to the strong vacuum ultraviolet multiplets $2s^22p^3\,{}^2D^o$–$2s^22p^23s\,{}^2D$, $2s^22p^3\,{}^2D^o$–$2s^22p^23s\,{}^2P$, and $2s^22p^3\,{}^2P^o$–$2s^22p^23s\,{}^2P$ at 1243, 1493, and 1743 Å, respectively, were measured by Goldbach *et al.* [6] using a wall stabilized arc method and more recently Goldbach *et al.* [7] used the same method to measure oscillator strengths of the $2s^22p^3\,{}^4S^o$–$2s^22p^23s\,{}^4P$, $2s^22p^3\,{}^4S^o$–$2s2p^4\,{}^4P$, $2s^22p^3\,{}^4S^o$–$2s^22p^24s\,{}^4P$, $2s^22p^3\,{}^4S^o$–$2s^22p^23d\,{}^4P$, $2s^22p^3\,{}^2D^o$–$2s^22p^23d\,{}^2F$, and $2s^22p^3\,{}^2D^o$–$2s^22p^24s\,{}^2P$ transitions. Goldbach and Nollez [8] measured oscillator strengths of seven weak multiplets in the 1300–1500 Å spectral range in emission using a wall-stabilized arc method. Lugger *et al.* [9] derived oscillator strengths from astrophysical observations. Musielok *et al.* [10] measured the relative transition probabilities of 100 lines of N I in the visible and near infrared spectral regions and normalized these to absolute value utilizing lifetime results. Zhu *et al.* [11] also measured relative transition probabilities of neutral nitrogen in emission with a wall-stabilized arc method. There have been several measurements of the radiative lifetimes of the $2s^22p^23s\,{}^4P$ and $2s2p^4\,{}^4P$ states of neutral nitrogen. Using the beam-foil method Chang [12], Dumont *et al.* [13], Kernahan *et al.* [14], Berry *et al.* [15], and Smith *et al.* [16] have measured the radiative lifetimes of these states. Brooks *et al.* [17], Hutchison [18], and Lawrence and Savage [19] also made these measurements using a phase-shift method. There are measurements of lifetimes by Mallow and Burns [20] using a pulsed beam, and Labuhn [21] using an arc method, and that of Lin *et al.* [22] who used a titration method. Bengtsson *et al.* [23], Catherinot and Sy [24], and Copeland *et al.* [25] obtained lifetimes of the $2p^23p\,{}^4S^o$ and $2p^23p\,{}^4D^o$ states with state selective laser excitation techniques.

Theoretical cross sections for elastic and inelastic scattering of electrons from atomic nitrogen have been reported by Berrington *et al.* [26] over an electron energy range from threshold to 35 eV. They performed three independent calculations by including 4 *LS* states $2s^22p^3\,{}^4S^o$, $^2D^o$, $^2P^o$, and $2s2p^4\,{}^4P$; 6 *LS* states $2s^22p^3\,{}^4S^o$, $^2D^o$, $^2P^o$, $2s2p^4\,{}^{4,2}P$ and ^2D; and 8 *LS* states $2s^22p^3\,{}^4S^o$, $^2D^o$, $^2P^o$, $2s2p^4\,{}^{4,2}P$, ^2D, ^2S, and $2p^5\,{}^2P^o$ in the close-coupling expansions using *R*-matrix method. Ramsbottom and Bell [27] also published cross sections over an incident electron energy range from threshold to 13.6 eV obtained in a 7-state close-coupling approximation. Ramsbottom and Bell [27] included three terms ($^4S^o$, $^2D^o$, and $^2P^o$) of the ground $2s^22p^3$ configuration together with four pseudostates to account for the polarizabilities of the $^4S^o$, $^2D^o$, and $^2P^o$ states. Thomas and Nesbet [28] used matrix variation method to calculate cross sections for the scattering of electrons from

TABLE I. Parameters of the radial functions of N I.

Orbital	Powers of r	Exponents	Coefficients	Orbital	Powers of r	Exponents	Coefficients
$1s$	1	6.457390	0.937794	$4p$	2	2.808764	0.718337
	1	11.172000	0.058489		3	5.042256	−0.061535
	2	1.364050	0.000930		4	1.676895	−1.087283
	2	1.897340	−0.001700		4	0.616302	0.505826
	2	3.252910	0.005740				
	2	5.082380	0.009569				
$2s$	1	6.457390	−0.216768	$5p$	2	2.967792	0.258382
	1	11.172000	−0.008460		3	0.639289	1.298512
	2	1.364050	0.179909		4	1.820905	−0.765207
	2	1.897340	0.674156		5	0.505623	−1.295951
	2	3.252910	0.312968				
	2	5.082380	−0.144969				
$3s$	1	5.719390	0.091925	$3d$	3	1.695071	0.073760
	2	3.757180	−0.086385		3	0.374905	0.985484
	3	2.822150	−0.264701				
	3	0.721460	1.014379				
$4s$	1	5.591291	0.034214	$4d$	3	2.625303	0.105301
	2	2.175704	−0.127504		3	0.841961	2.489580
	3	0.805945	0.271071		4	1.103713	−1.717963
	4	0.379135	−1.147067		4	0.285117	−0.756023
	4	0.769198	0.312588				
$5s$	1	4.570678	0.293971	$5d$	3	2.232180	2.620393
	2	1.701446	−2.162652		3	2.135817	−1.712292
	3	1.585264	2.785534		4	0.709284	−0.488994
	4	0.888186	−1.042151		4	0.276778	0.424040
	5	0.415284	0.312588				
$2p$	2	1.180284	0.074532	$4f$	4	0.762250	1.000000
	2	1.752549	0.628113				
	2	2.899459	0.330684				
	2	6.479618	0.021095				
$3p$	2	4.252280	0.022281				
	2	2.166810	0.123812				
	3	2.265470	0.030137				
	3	0.538850	−1.006630				

atomic nitrogen and Burke *et al.* [29] used a 6-state approximation in the framework of *R*-matrix method. Henry *et al.* [30] included $2s^22p^3\,{}^4S^o$, ${}^2D^o$, and ${}^2P^o$ states in the close-coupling expansion while Ormonde *et al.* [31] considered these plus some states of higher configurations. Henry *et al.* [30] and Ormonde *et al.* [31] represented target states by single configuration. The measurement of the differential cross sections (DCS) for the forbidden ${}^4S^o$-${}^2D^o$ transition ($\lambda = 5200$ Å) is reported by Yang and Doering [32] at incident energies from 5 to 30 eV. The measured DCS are integrated over scattering angles to obtain the integral cross sections (ICS) as a function of incident energy.

We calculated energy levels, oscillator strengths, and radiative lifetimes of the excited states using the CI wave functions. The LS states of the configurations $2s^22p^3$, $2s2p^4$, $2s^22p^23s$, $2s^22p^23p$, $2s^22p^23d$, and $2s^22p^24s$ are considered in these calculations. The differential and integral cross sections of the forbidden ${}^4S^o$-${}^2D^o$ transition for the scattering of electrons from atomic nitrogen are calculated by including 11 LS states ($2s^22p^3\,{}^4S^o$, ${}^2D^o$, ${}^2P^o$, $2s2p^4\,{}^4P$, $2s^22p^23s\,{}^4P$, ${}^2P$, $2s^22p^23p\,{}^4D^o$, ${}^4P^o$, ${}^4S^o$, $2s^22p^23d\,{}^4P$, and $2s^22p^24s\,{}^4P$) in the close-coupling expansion and by the use of *R*-matrix method [33].

II. METHODS OF CALCULATION

The atomic state CI wave functions are written in the form,

$$\Psi(LS) = \sum_{i=1}^{M} a_i \Phi_i(\alpha_i LS), \tag{1}$$

where each single configuration function Φ_i is constructed from orbitals whose angular momenta are coupled, as specified by α_i, to form a total L and S common to all M configurations. The analytical form of the one-electron radial function is given by

$$P_{n,l}(r) = \sum_{j=1}^{k} C_{jnl} N_{jnl} r^{jnl} \exp\{-\zeta_{jnl} r\}, \tag{2}$$

TABLE II. Excited-state energies (in au) of N I relative to the ground state.

Index	State	This work	Experiment [a]	Hibbert [b]	Tong [c]
1	$2s^2 2p^3\,{}^4S^o$	0.00	0.00	0.00	0.00
2	$2s^2 2p^3\,{}^2D^o$	0.10464	0.08760	0.12780	
3	$2s^2 2p^3\,{}^2P^o$	0.15017	0.13140	0.15778	
4	$2s^2 2p^2({}^3P)3s\,{}^4P$	0.38346	0.37971	0.39992	0.38220
5	$2s^2 2p^2({}^3P)3s\,{}^2P$	0.39676	0.38361	0.41533	
6	$2s2p^4\,{}^4P$	0.41089	0.40155	0.41511	0.40324
7	$2s^2 2p^2({}^3P)3p\,{}^2S^o$	0.42865	0.42639	0.44811	
8	$2s^2 2p^2({}^3P)3p\,{}^4D^o$	0.43433	0.43212	0.45318	0.43698
9	$2s^2 2p^2({}^3P)3p\,{}^4P^o$	0.43701	0.43518	0.45613	0.43825
10	$2s^2 2p^2({}^3P)3p\,{}^4S^o$	0.44334	0.44083	0.46213	0.44422
11	$2s^2 2p^2({}^3P)3p\,{}^2D^o$	0.44493	0.44121	0.46402	
12	$2s^2 2p^2({}^3P)3p\,{}^2P^o$	0.44917	0.44558	0.46951	
13	$2s^2 2p^2({}^3P)4s\,{}^4P$	0.47254	0.47247	0.49269	0.47670
14	$2s^2 2p^2({}^3P)4s\,{}^2P$	0.47591	0.47477	0.49526	0.48089
15	$2s^2 2p^2({}^3P)3d\,{}^2P$	0.47407	0.47672	0.49698	
16	$2s^2 2p^2({}^3P)3d\,{}^4F$	0.47424	0.47714	0.49723	
17	$2s^2 2p^2({}^3P)3d\,{}^2F$	0.47691	0.47774	0.49786	
18	$2s^2 2p^2({}^3P)3d\,{}^4P$	0.47648	0.47846	0.49784	0.48233
19	$2s^2 2p^2({}^3P)3d\,{}^4D$	0.47628	0.47846	0.49854	0.48213
20	$2s^2 2p^2({}^3P)3d\,{}^2D$	0.47679	0.47903	0.49923	

[a] Reference [37].
[b] Reference [3].
[c] Reference [4].

with $k \geqslant n\text{-}l$ and the normalization factor,

$$N_{jnl} = \frac{[2\zeta_{jnl}]^{I_{jnl}+1/2}}{[(2I_{jnl})!]^{1/2}}, \tag{3}$$

where C_{jnl}, ζ_{jnl}, and I_{jnl} are the expansion coefficients, exponents, and powers of r, respectively. For a given set of configuration state functions, the coefficients a_i in Eq. (1) are components of the eigenvector of the Hamiltonian matrix with typical element,

$$H_{ij} = \langle \Psi_i | H | \Psi_j \rangle, \tag{4}$$

where H represents the nonrelativistic Hamiltonian operator. The Hamiltonian matrix can be diagonalized to give $E_1 < E_2 < \cdots < E_M$. From the Hylleraas-Undheim-MacDonald theorem, we have

$$E_k > E_k^{exact}. \tag{5}$$

The upper bound property of Eq. (5) can be used to determine the optimum values of the parameters C_{jnl} and ζ_{jnl} in Eq. (2), subject to the orthonormality condition,

$$\int_0^\infty P_{nl}(r) P_{n'l}(r)\,dr = \delta_{nn'}. \tag{6}$$

The total wave function representing the scattering of electrons by atomic nitrogen is expanded as [34]

$$\Psi_k = A \sum_{ij} c_{ijk} \bar{\Phi}(1,2,\ldots,7,r_8,\sigma_8) u_{ij}(r_8) + \sum_j d_{jk} \phi_j(1,2,\ldots,8), \tag{7}$$

where the functions $\bar{\Phi}$ are formed by coupling the multiconfigurational functions Φ_i of the target bound states with the spin-angle functions of the scattered electron, and the u_{ij} are the numerical basis functions for the scattered electron. The operator A antisymmetrizes the wave function and c_{ijk} and d_{jk} are expansion coefficients determined by diagonalizing the (N+1)-electron Hamiltonian. The functions ϕ_j in Eq. (7) are of bound-state type and are included to compensate for the imposition of orthogonality conditions. Additional functions ϕ_j are included to allow for the short-range electron correlation effects. We included 44 continuum orbitals in each channel, which give good convergence for energies up to 100 eV. Application of a variational principle leads to a set of coupled integrodifferential equations, which are solved numerically by the use of the R-matrix method [34]. A boundary radius $r = 36.8$ a.u. is introduced, which is large compared with the mean radii of the target orbitals. At each incident electron energy, calculations are performed for eleven values of angular momenta $L = 0$–10, which gave converged cross sections for the forbidden ${}^4S^o$-${}^2D^o$ transition. We adjusted the calculated energies of the target states to reproduce the observed values in our scattering calculation. The diagonal elements of the inner region Hamiltonian matrix are also adjusted before diagonalization.

Thirteen orthogonal one-electron orbitals $1s$, $2s$, $2p$, $3s$,

TABLE III. Oscillator strengths of dipole-allowed transitions between states of quartet symmetry in N I.

			Other calculations						
	This work		Tong[a]		Hibbert[b]		Bell[c]		
Transition	f_L	f_V	f_L	f_V	f_L	f_V	f_L	f_V	Experiment
$2p^3\,{}^4S^o$–$3s\,{}^4P$	0.294	0.320	0.284	0.296	0.251	0.272	0.262	0.274	0.271[d]; 0.266[e]
$2p^3\,{}^4S^o$–$2p^4\,{}^4P$	0.064	0.078	0.066	0.069	0.081	0.111	0.087	0.095	0.078[f]; 0.080; 0.085[g]
$2p^3\,{}^4S^o$–$4s\,{}^4P$	0.025	0.025	0.025	0.026	0.032	0.030	0.026	0.026	0.030[e]; 0.027[g]
$2p^3\,{}^4S^o$–$3d\,{}^4P$	0.078	0.065	0.076	0.076	0.066	0.060	0.078	0.069	0.067[e]; 0.075[g]
$3p\,{}^4S^o$–$4s\,{}^4P$	0.098	0.152	0.146	0.157	0.089	0.156	0.142	0.164	
$3p\,{}^4S^o$–$3d\,{}^4P$	0.919	0.954	1.010	1.022	0.751	0.893	1.02	0.849	
$3s\,{}^4P$–$3p\,{}^4S^o$	0.087	0.092	0.094	0.094	0.107	0.089			0.102[h]
$2p^4\,{}^4P$–$3p\,{}^4S^o$	0.043	0.036	0.034	0.042	0.030	0.042			
$3s\,{}^4P$–$3p\,{}^4D^o$	0.430	0.474	0.429	0.440	0.490	0.475			0.455[h]
$2p^4\,{}^4P$–$3p\,{}^4D^o$	0.079	0.102	0.071	0.081	0.052	0.057			
$3p\,{}^4D^o$–$4s\,{}^4P$	0.128	0.153	0.148	0.163	0.165	0.143			
$3p\,{}^4D^o$–$3d\,{}^4P$	0.013	0.021	0.014	0.019	0.031	0.028			
$3s\,{}^4P$–$3p\,{}^4P^o$	0.290	0.291	0.283	0.287	0.318	0.277			0.304[h]
$2p^4\,{}^4P$–$3p\,{}^4P^o$	0.027	0.042	0.028	0.027	0.015	0.014			
$3p\,{}^4P^o$–$4s\,{}^4P$	0.171	0.212	0.198	0.218	0.211	0.205			
$3p\,{}^4P^o$–$3d\,{}^4P$	0.197	0.178	0.204	0.203	0.231	0.221			
$3p\,{}^4D^o$–$3d\,{}^4F$	0.780	0.856	0.765	0.801	0.827	0.786			
$3p\,{}^4D^o$–$3d\,{}^4D$	0.143	0.133	0.137	0.136	0.139	0.123			
$3p\,{}^4P^o$–$3d\,{}^4D$	0.689	0.759	0.690	0.713	0.684	0.682			

[a] Reference [4].
[b] Reference [2].
[c] Reference [5].
[d] Reference [6].
[e] Reference [9].
[f] Reference [16].
[g] Reference [7].
[h] Reference [11].

$3p$, $3d$, $4s$, $4p$, $4d$, $4f$, $5s$, $5p$, and $5d$ are used in our calculation. The $1s$, $2s$, and $2p$ radial functions are chosen as the Hartree-Fock functions of the $2s^22p^3\,{}^4S^o$ ground state of N I given by Clementi and Roetti [35] and the $2p$ function has been reoptimized on the state $2s^22p^23s\,{}^4P$. The $2p$ and other radial functions have been obtained with the general nonrelativistic structure code CIV3 of Hibbert [36]. The radial part of each orbital is expressed in analytical form as a sum of Slater-type orbitals. The exponents and coefficients are determined variationally. The coefficients are also subjected to orthonormality conditions. The $3s$, $4s$, $3p$, and $3d$ functions are chosen of spectroscopic type and are optimized on the excited states $2p^23s\,{}^4P$, $2p^24s\,{}^4P$, $2p^23p\,{}^4D^o$, and $2p^23d\,{}^4P$, respectively. There is strong interaction between the $2p^24s\,{}^4P$ and $2p^23d\,{}^4P$ states because of their proximity. In order to represent these states accurately it is necessary to obtain flexible spectroscopic functions on these states. The $4p$, $4d$, $4f$, $5s$, $5p$, and $5d$ functions are correlation type. It is necessary to use the correlation functions in addition to spectroscopic functions so that a single set of orthogonal functions can represent all the energy states. The $4p$ function is chosen as a correction to $2p$ in the ground state and is optimized on this state. The $5p$ function is chosen to improve the flexibility of the $3p$ function and is optimized on the $2p^23p\,{}^2D^o$ state. The $5s$ and $5d$ functions are chosen to account for the polarizability of the ground state. The $4d$ and $4f$ functions are chosen to improve the energies of the $2s2p^4\,{}^4P$ and $2s^22p^23d\,{}^4P$ states, respectively. The parameters of the optimized radial functions are given in Table I.

III. RESULTS AND DISCUSSION

A. Excitation energies and oscillator strengths

In order to test the convergence of the CI expansion for different LS symmetries, we carried out several test calculations. All configurations with weight more than 0.003 are retained in our final calculation. These CI wave functions are then used to calculate excitation energies and oscillator strengths. The calculated excitation energies of the various states relative to the $2s^22p^3\,{}^4S^o$ ground state of N I are presented in Table II and these are compared with the experimental energies [37] and the theoretical energies reported by Tong *et al.* [4] and Hibbert *et al.* [2].

The present calculated energies agree to better than 1% with the measured values for most states. The largest discrepancies are for the $2s^22p^3\,{}^2D^o$ and $2s^22p^3\,{}^2P^o$ states where the calculated results are, respectively, 19% and 14% larger than the measured values. Our calculation agrees very well with the CI calculation of Hibbert *et al.* [2] and the multiconfiguration Hartree-Fock (MCHF) calculation of Tong *et al.* [4]. The energy ordering of the $2s^22p^24s\,{}^2P$, $2s^22p^23d\,{}^{2,4}P$, ${}^{2,4}F$, ${}^4D$, and ${}^2D$ states is not in agreement with the experiment. The energy gap between these states is very small.

The length and velocity forms of oscillator strengths for dipole-allowed transitions between states of quartet and doublet symmetries are listed in Tables III and IV. In our calculation of oscillator strengths we have adjusted the diagonal elements of the Hamiltonian matrices to produce energy splittings between states as close as possible to experimental

TABLE IV. Oscillator strengths of dipole-allowed transition between states of doublet symmetry in N I.

Transition	This work		Other calculation[a]		Experiment
	f_L	f_V	f_L	f_V	
$2p^3\,{}^2D^o - 3s\,{}^2P$	0.077	0.074	0.075	0.076	0.071[b]
$2p^3\,{}^2D^o - 4s\,{}^2P$	0.019	0.014	0.005	0.015	0.013[c]
$2p^3\,{}^2D^o - 3d\,{}^2P$	0.00004	0.0004	0.017	0.002	
$2p^3\,{}^2D^o - 3s\,{}^2D$	0.082	0.079	0.082	0.086	0.083[b]
$2p^3\,{}^2D^o - 3d\,{}^2D$	0.003	0.003	0.015	0.005	
$2p^3\,{}^2D^o - 3d\,{}^2F$	0.065	0.074	0.045	0.031	0.032[c]
$3p\,{}^2D^o - 3d\,{}^2D$	0.124	0.140	0.121	0.140	
$3p\,{}^2D^o - 4s\,{}^2P$	0.106	0.198	0.101	0.196	
$3p\,{}^2D^o - 3d\,{}^2P$	0.038	0.061	0.042	0.058	
$3p\,{}^2D^o - 3d\,{}^2F$	0.682	0.863	0.672	0.806	
$2p^3\,{}^2P^o - 3s\,{}^2P$	0.068	0.079	0.066	0.056	0.061[b]
$2p^3\,{}^2P^o - 4s\,{}^2P$	0.008	0.003			0.003[d]
$2p^3\,{}^2P^o - 3d\,{}^2P$	0.029	0.027	0.020	0.013	0.020[d]
$2p^3\,{}^2P^o - 3s\,{}^2D$	0.025	0.022	0.028	0.025	
$2p^3\,{}^2P^o - 3d\,{}^2D$	0.033	0.040	0.061	0.033	0.037[d]
$3p\,{}^2P^o - 4s\,{}^2P$	0.284	0.377	0.214	0.428	
$3p\,{}^2P^o - 3d\,{}^2P$	0.095	0.078	0.089	0.089	
$3p\,{}^2P^o - 3d\,{}^2D$	0.666	0.701	0.568	0.772	
$3s\,{}^2P - 3p\,{}^2S^o$	0.109	0.061	0.091	0.071	
$3s\,{}^2P - 3p\,{}^2D^o$	0.696	0.472	0.590	0.662	
$3s\,{}^2P - 3p\,{}^2P^o$	0.403	0.306	0.364	0.354	
$3p\,{}^2S^o - 4s\,{}^2P$	0.001	0.001	0.007	0.002	
$3p\,{}^2S^o - 3d\,{}^2P$	1.061	0.971	1.205	0.919	

[a] Reference [2].
[b] Reference [7].
[c] Reference [6].
[d] Reference [8].

TABLE V. Radiative lifetimes (ns) of excited states.

Method	Reference	Lifetimes/excited states			
		$3s\,{}^4P$	$2p^4\,{}^4P$	$3p\,{}^4S^o$	$3p\,{}^4D^o$
		Experiment			
Laser excitation	[23]			26.0±1.5	44±2
Laser excitation	[24]			23.3±2.3	
Laser excitation	[25]				43±3
Arc	[6]	2.39			
Arc	[21]	1.85±0.74	4.3±2.2		
Beam-foil	[12]	2.27	3.18		
Beam-foil	[13]	2.35±0.23	7.3±0.7		
Beam-foil	[14]		6.80±0.30		
Beam-foil	[16]		7.4±0.4		
Beam-foil	[15]	2.4±0.1	7.0±0.2		
Pulsed-beam	[20]	5.5±1.5			
Phase-shift	[17]	2.4±0.2			
Phase-shift	[18]	2.2±0.4	9.9±1.0		
Phase-shift	[19]	2.5±0.3	7.2±0.7		
Titration	[22]	3.0±0.7			
		Theoretical			
CIV3	This Work	2.20	9.10	26.5	41.3
CIV3	[2]	2.59	7.14	23.3	37.2
CIV3	[3]	2.32	8.26		
MCHF	[4]	2.28	8.82		

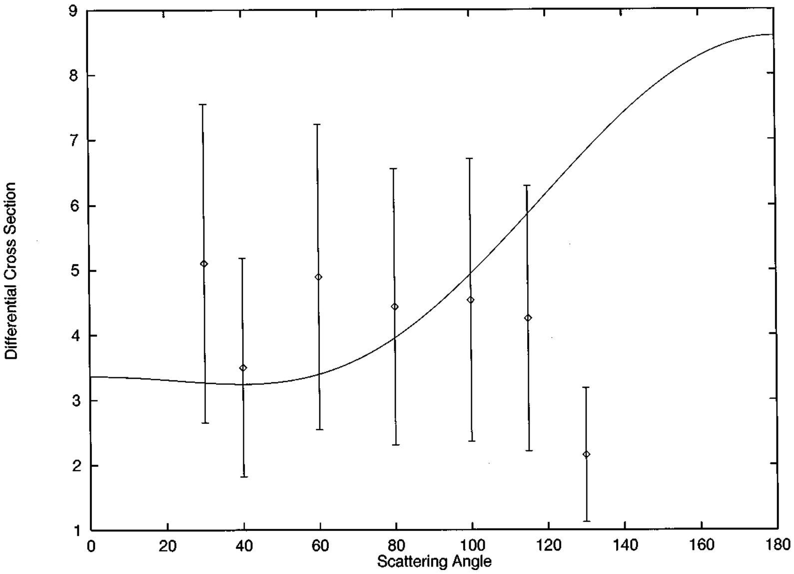

FIG. 1. Differential cross sections (10^{-18} cm^2/sr) for the $^4S^o$-$^2D^o$ transition in atomic nitrogen as a function of scattering angle (deg) at the incident electron energy 5 eV. Solid line: present theoretical results; diamonds: measured values [32].

values. These adjustments also caused some changes in the weights of eigenvectors. These changes were significant for those cases where mixing between states of main configurations was strong. Thus oscillator strengths of some transitions are significantly changed from the values obtained with theoretical transition energies. Brage and Hibbert [38] have discussed the justification of this procedure. Transitions between the terms of the ground $2s^22p^3$ and the excited $2s^22p^23s$, $2s2p^4$, $2s^22p^23p$, $2s^22p^23d$, and $2s^22p^24s$ configurations are shown and these are compared with the calculations of Hibbert *et al.* [2], Tong *et al.* [4], and the various measurements. We have converted LSJ oscillator strengths of Hibbert *et al.* [2] to multiplet oscillator strengths to compare with our results in Tables III and IV. The results of Robinson and Hibbert [1] are within a few per cent of Hibbert *et al.* [2] and are not given in Table III. The agreement between the present length and velocity forms and with other theoretical calculations and experiments is generally within 25% for most transitions given in Table III. Goldbach *et al.* [6] estimated uncertainties between 12% and 20% in their measured oscillator strengths and Goldbach and Nollez [8] and Goldbach *et al.* [7] claimed an accuracy of better than 10% for their results. Our results of oscillator strengths agree well with the CI calculations of Hibbert *et al.* [2], the MCHF calculation of Tong *et al.* [4], and the *R*-matrix calculation of Bell and Berrington [5] for most transitions. The worst agreement is for the $2s^22p^23p\,^4S^o$–$2s^22p^24s\,^4P$, $2s2p^4\,^4P$–$2s^22p^23p\,^4P^o$, and $2s^22p^23p\,^4D^o$ –$2s^22p^23d\,^4P$ transitions. The results for transitions involving the $2s2p^4\,^4P$ state are sensitive to the choice of wave functions and electron correlation effects.

For dipole-allowed transitions among the states of doublet symmetry, the present results normally agree with the calculation of Hibbert *et al.* [2] and measured values of Goldbach *et al.* [6,7] and Goldbach and Nollez [8] for many transitions, except for transitions where oscillator strengths are small and for the $2p^3\,^2D^o$–$3d\,^2F$ transition. In case of smaller oscillator strengths there may be some delicate can-

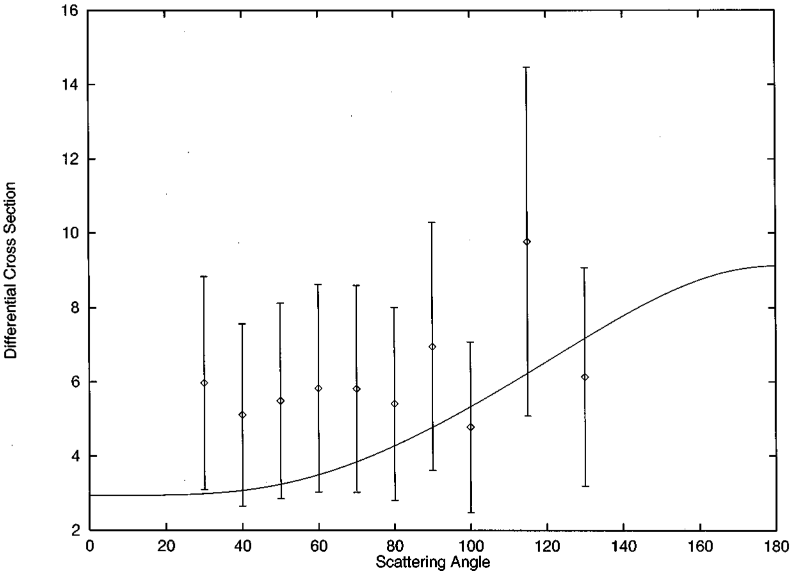

FIG. 2. Differential cross sections (10^{-18} cm^2/sr) for the $^4S^o$-$^2D^o$ transition in atomic nitrogen as a function of scattering angle (deg) at the incident electron energy 7 eV. Notations are the same as in Fig. 1.

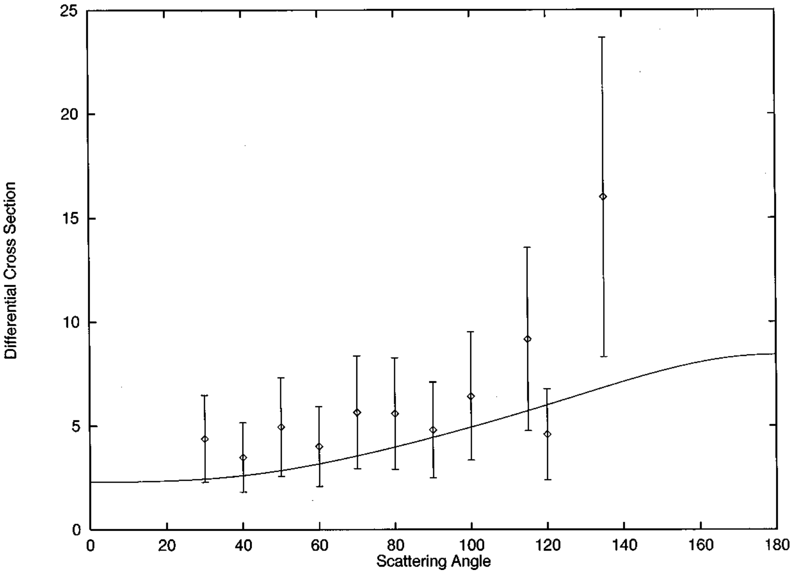

FIG. 3. Differential cross sections (10^{-18} cm^2/sr) for the $^4S^o$-$^2D^o$ transition in atomic nitrogen as a function of scattering angle (deg) at the incident electron energy 8 eV. Notations are the same as in Fig. 1.

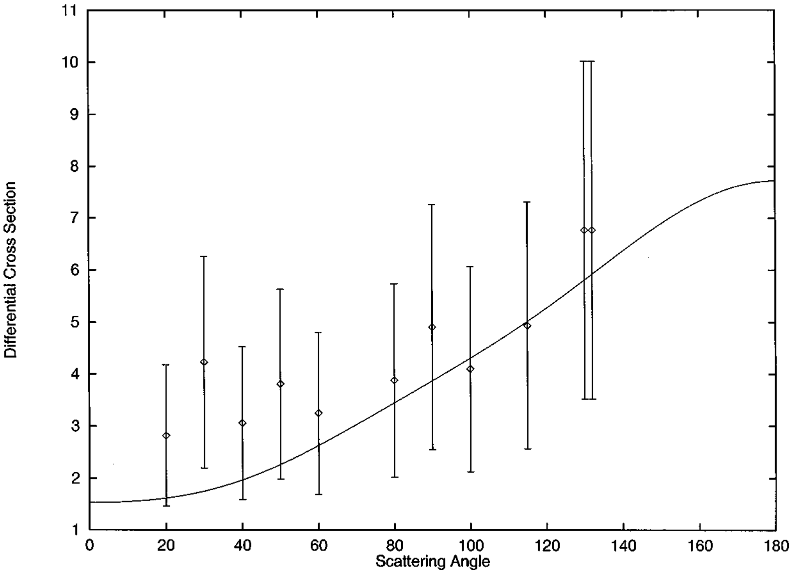

FIG. 4. Differential cross sections (10^{-18} cm^2/sr) for the $^4S^o$-$^2D^o$ transition in atomic nitrogen as a function of scattering angle (deg) at the incident electron energy 10 eV. Notations are the same as in Fig. 1.

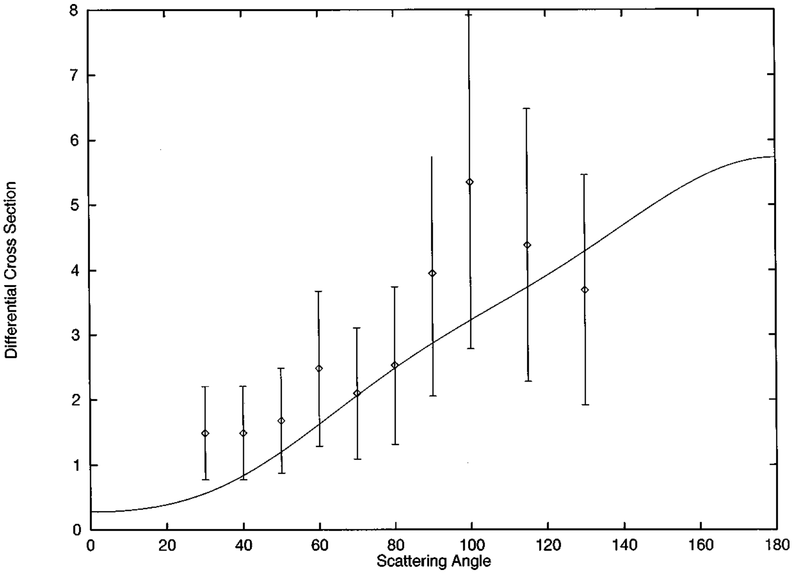

FIG. 5. Differential cross sections (10^{-18} cm^2/sr) for the $^4S^o$-$^2D^o$ transition in atomic nitrogen as a function of scattering angle (deg) at the incident electron energy 15 eV. Notations are the same as in Fig. 1.

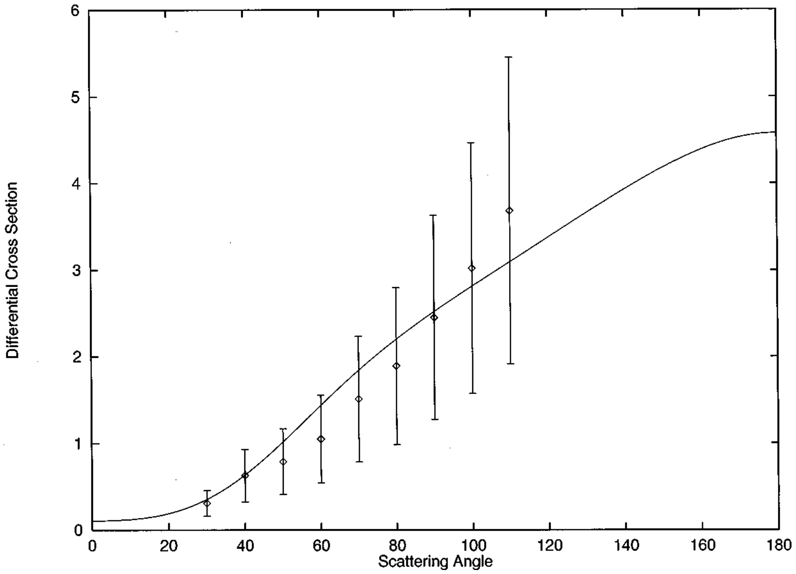

FIG. 6. Differential cross sections (10^{-18} cm^2/sr) for the $^4S^o$-$^2D^o$ transition in atomic nitrogen as a function of scattering angle (deg) at the incident electron energy 20 eV. Notations are the same as in Fig. 1.

cellations leading to discrepancies.

Since many experimental publications report radiative lifetimes, we have given lifetimes in Tables V to compare our results with these measurements. The experimental lifetime of the $2s^22p^23s\,^4P$ state range from 1.85 to 3.0 ns. Our calculated value of 2.20 ns agrees well with the most recent of these experiments [6]. Our calculation is also in very good agreement with the calculated value of Tong *et al.* [4]. For the $2s2p^4\,^4P$ state we are larger than the calculation of Hibbert *et al.* [2] and Tong *et al.* [4] by approximately 22% and 3%, respectively. For the $2s^22p^23p\,^4S^o$ and $2s^22p^23p\,^4D^o$ excited states our calculated lifetimes agree well with the calculation of Hibbert *et al.* [2] and measured values of Bengtsson *et al.* [23], Catherinot and Sy [24], and Copeland *et al.* [25].

B. Differential and integral cross sections

Electron-impact excitation differential cross sections for the forbidden $^4S^o$-$^2D^o$ transition in atomic nitrogen are displayed in Figs. 1–7 over an incident electron energy range from 5 to 30 eV and in the angular range from 0 to 180°. These are compared with the measurements of Yang and Doering [32]. The theoretical cross sections are shown by the full curve and the open diamonds represent the measured values of Yang and Doering [32] who reported DCS in the angular range 20–135°. The estimated uncertainties in the measured DCS are $\pm 48\%$. We have plotted the averages of three sets of measured DCS in these figures. Our theoretical DCS at all energies are peaked in the backward direction and this trend is in agreement with the experiment. This is the expected behavior of a spin-changing forbidden transition as at low energies the spin-changing forbidden transitions are dominated by exchange interaction at large scattering angles. The peak in the backward direction becomes stronger as the incident electron energy increases. Our calculated DCS are well within the experimental errors at most scattering angles for the incident energies 5 to 20 eV but at 30 eV our results are larger than the experiment at many scattering angles.

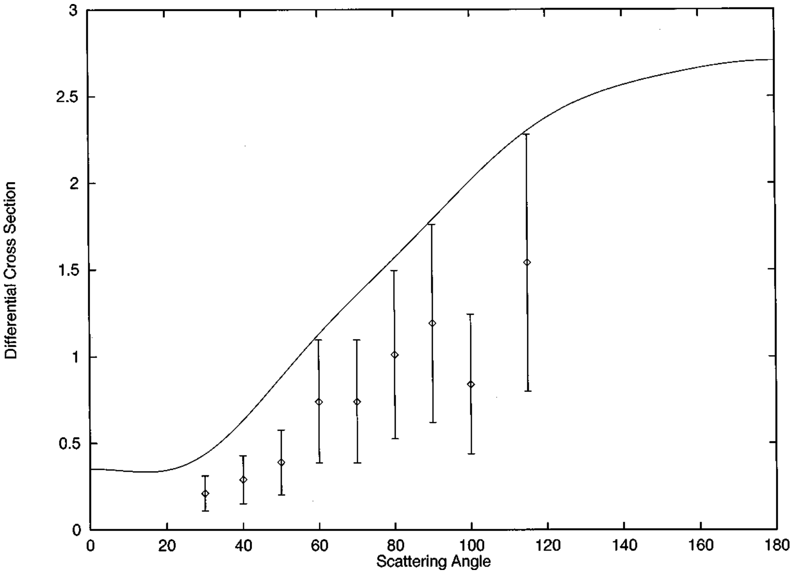

FIG. 7. Differential cross sections (10^{-18} cm^2/sr) for the $^4S^o$-$^2D^o$ transition in atomic nitrogen as a function of scattering angle (deg) at the incident electron energy 30 eV. Notations are the same as in Fig. 1.

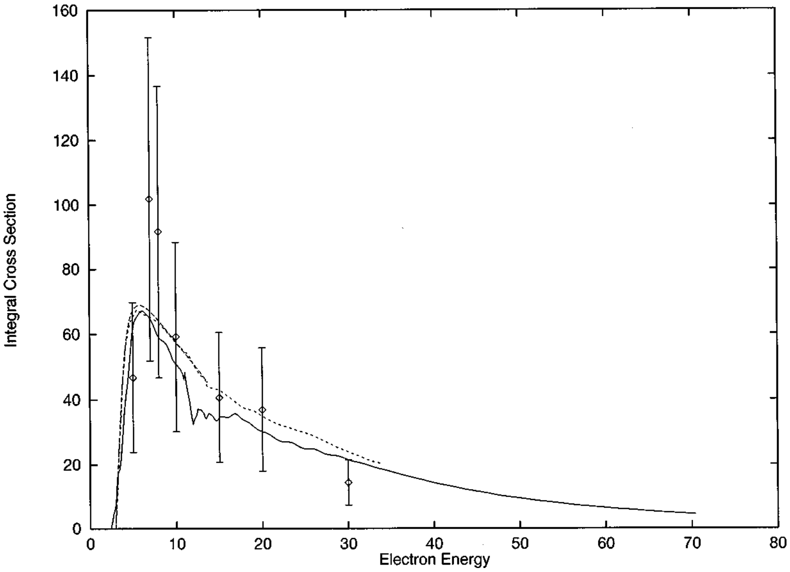

FIG. 8. Integral cross sections (10^{-18} cm^2) for the $^4S^o$-$^2D^o$ transition in atomic nitrogen as a function of the energy (eV) of the incident electron. Solid line: present 11-state *R*-matrix results; short-dashed line: 8-state *R*-matrix calculation of Berrington *et al.* [26]; long-dashed line: 7-state *R*-matrix calculation of Ramsbottom and Bell [27].

The integral-excitation cross sections for the $^4S^o$-$^2D^o$ transition are plotted in Fig. 8 where they are compared with the measurement of Yang and Doering [32] and with the calculations of Berrington *et al.* [26] and Ramsbottom and Bell [27]. Again the average of three sets of measured ICS at each energy is plotted in Fig. 8. The agreement between the present calculated results and the measurements of Yang and Doering [32] is excellent at all incident-electron energies. The present theoretical calculation predicts a peak at around 6.12 eV, which is in excellent agreement with the calculations of Berrington *et al.* [26] and Ramsbottom and Bell [27]. The peak in the meaured cross sections seem to occur at slightly higher energy and has the value 96 ± 32 $\times10^{-18}$ cm^2, which they obtained by averaging the peak cross sections at 7 and 8 eV. The calculated peak cross section is 67.25×10^{-18} cm^2. There is also an overall good agreement between the three calculations. Berrington *et al.* [26] noted a dip in their cross sections due to a cusp associated with the opening of channel coupled to the $2s2p^4\,{}^4P$ threshold. In our calculation we included $2p^23s\,{}^4P$, ^2P, $2s2p^4\,{}^4P$, $2p^23p\,{}^2S^o$, $^4D^o$, $^4P^o$, $^4S^o$, $2p^24s\,{}^4P$, and $2p^23d\,{}^4P$ states with threshold energies in the 10.3–13.0-eV region. Some structure in our cross sections in this energy region is due to coupling to additional states not considered by earlier calculations of Berrington *et al.* [26] and Ramsbottom and Bell [27]. The structure above 13.0 eV is due to pseudoresonances, which arise in our calculation because of the use of pseudo-orbitals. The *T*-matrix averaging procedure of Burke *et al.* [39] can be used to smooth over pseudoresonances. We have made no attempt in our work to smooth over these resonances. Alternatively, the pseudoresonance structure can also be reduced by including pseudostates with thresholds in this energy region in the close-coupling expansion together with physical states as described by Bartschat *et al.* [40] and this will be the subject of future investigation.

IV. CONCLUSION

We have presented an extensive CI calculation of energy levels, oscillator strengths, and radiative lifetimes of excited states. We considered 20 low-lying *LS* states belonging to the $2s^22p^3$, $2s2p^4$, $2s^22p^23s$, $2s^22p^23p$, $2s^22p^23d$, and $2s^22p^24s$ configurations of N I in the structure calculation and 11 *LS* states in our scattering calculation. Theoretical integral and differential cross sections for electron-impact excitation of the $^4S^o$-$^2D^o$ transition in atomic nitrogen, which give rise to prominent emission feature at 5200 Å in the aurora, is reported. The theoretical cross sections are normally in very good agreement with the measurement of Yang and Doering [32] and display the characteristic shape of the spin-changing forbidden transition.

ACKNOWLEDGMENTS

This research was supported by NASA Grant No. NAG5-6889. The computational work was carried out on the JPL/Caltech Cray supercomputer.

---

[1] D. J. R. Robinson and A. Hibbert, J. Phys. B **30**, 4813 (1997).
[2] A. Hibbert, E. Biémont, M. Godefroid, and N. Vaeck, Astron. Astrophys., Suppl. Ser. **88**, 505 (1991).
[3] A. Hibbert, P. L. Dufton, and F. P. Keenan, Mon. Not. R. Astron. Soc. **213**, 721 (1985).
[4] M. Tong, C. Froese Fischer, and L. Sturesson, J. Phys. B **27**, 4819 (1994).
[5] K. L. Bell and K. A. Berrington, J. Phys. B **24**, 933 (1991).
[6] C. Goldbach, M. Martin, G. Nollez, P. Plombeur, J.-P. Zimmermann, and D. Babic, Astron. Astrophys. **161**, 47 (1986).
[7] C. Goldbach, T. Lüdtke, M. Martin, and G. Nollez, in *Proceedings of the 4th International Colloquium on Atomic Spectra and Oscillator Strengths for Astrophysical and Laboratory Plasmas, Gaithersburg,* edited by J. Sugar and D. Leckrone (NIST, Gaithersburg, MD, 1993), p. 77.
[8] C. Goldbach and G. Nollez, Astron. Astrophys. **201**, 189 (1988).
[9] P. M. Lugger, D. G. York, and T. Blanchard, Astrophys. J. **224**, 1059 (1978).

[10] J. Musielok, W. L. Wiese, and G. Veres, Phys. Rev. A **51**, 3588 (1995).

[11] Q. Zhu, J. M. Bridges, T. Hahn, and W. L. Wiese, Phys. Rev. A **40**, 3721 (1989).

[12] W.-W. Chang, Astrophys. J. **211**, 300 (1977).

[13] P. D. Dumont, E. Biémont, and N. Grevesse, J. Quant. Spectrosc. Radiat. Transf. **14**, 1127 (1974).

[14] J. A. Kernahan, A. E. Livingston, and E. H. Pinnington, Can. J. Phys. **52**, 1895 (1974).

[15] H. G. Berry, W. S. Bickel, S. Banskin, J. Désesquelles, and R. M. Schectman, J. Opt. Soc. Am. **61**, 947 (1971).

[16] H. W. Smith, J. Bromander, L. J. Curtis, and R. Buchta, Phys. Scr. **2**, 211 (1970).

[17] N. H. Brooks, D. Rohrich, and H. W. Smith, Astrophys. J. **214**, 328 (1977).

[18] R. B. Hutchison, J. Quant. Spectrosc. Radiat. Transf. **11**, 81 (1971).

[19] G. M. Lawrence and G. D. Savage, Phys. Rev. **141**, 61 (1966).

[20] J. V. Mallow and J. Burns, J. Quant. Spectrosc. Radiat. Transf. **12**, 1081 (1971).

[21] F. Labuhn, Z. Naturforsch. **20a**, 998 (1965).

[22] C. Lin, D. A. Parkes, and F. Kaufman, J. Chem. Phys. **53**, 3896 (1970).

[23] G. J. Bengtsson, J. Larsson, S. Svanberg, and D. D. Wang, Phys. Rev. A **45**, 2712 (1992).

[24] A. Catherinot and A. Sy, Phys. Rev. A **20**, 1511 (1979).

[25] R. A. Copeland, J.-B. Jeffries, A. P. Hickman, and D. R. Crossley, J. Chem. Phys. **86**, 4876 (1987).

[26] K. A. Berrington, P. G. Burke, and W. D. Robb, J. Phys. B **8**, 2500 (1975).

[27] C. A. Ramsbottom and K. L. Bell, Phys. Scr. **50**, 666 (1994).

[28] L. D. Thomas and R. K. Nesbet, Phys. Rev. A **12**, 2369 (1975).

[29] P. G. Burke, K. A. Berrington, M. Le Dourneuf, and Vo Ky Lan, J. Phys. B **7**, L531 (1974).

[30] R. J. W. Henry, P. G. Burke, and A. M. Sinfailam, Phys. Rev. **178**, 218 (1969).

[31] S. Ormonde, K. Smith, B. W. Torres, and A. R. Davies, Phys. Rev. A **8**, 282 (1973).

[32] J. Yang and J. P. Doering, J. Geophys. Res. **101**, 765 (1996).

[33] P. G. Burke and W. D. Robb, Adv. At. Mol. Phys. **11**, 143 (1975).

[34] K. A. Berrington, P. G. Burke, K. Butler, M. J. Seaton, P. J. Storey, K. T. Taylor, and Y. Yu, J. Phys. B **20**, 6379 (1987).

[35] E. Clementi and C. Roetti, At. Data Nucl. Data Tables **14**, 177 (1974).

[36] A. Hibbert, Comput. Phys. Commun. **9**, 141 (1975).

[37] C. E. Moore, *Atomic Energy Levels and Multiplet Tables*, Natl. Bur. Stand. (U.S.) Circ. No. 3 (U.S. GPO, Washington, D.C., 1975), Sec. 5.

[38] T. Brage and A. Hibbert, J. Phys. B **22**, 713 (1989).

[39] P. G. Burke, K. A. Berrington, and C. V. Sukumar, J. Phys. B **14**, 289 (1981).

[40] K. Bartschat, P. G. Burke, and M. P. Scott, J. Phys. B **29**, L769 (1996).